

Controlling Sensor Density using Mobility

Bin Zhang and Gaurav S. Sukhatme
Center For Embedded Networked Sensing (CENS)
Computer Science Department
University of Southern California,
Los Angeles, CA, 90089-0781, USA
binz@usc.edu, gaurav@usc.edu

Abstract

We present a distributed deployment algorithm for a mobile sensor network which is able to deploy sensor nodes in a distribution proportional to a scalar field. The algorithm randomly partitions space into sufficiently small neighborhoods at each iteration. Within each neighborhood a redistribution process directed by a cluster head is enacted. We prove that after sufficiently many iterations, the distribution of nodes approaches the desired profile in the overall region. The algorithm is scalable to large network sizes, and is not restricted to planar domains. We show experimentally that the algorithm is noise tolerant.

1. Introduction

Environmental sampling [2, 17] is rapidly becoming a focus of attention as a viable application of sensor networks. In such applications, the distribution of sensor nodes has considerable effect on the utility of the sensor network. Research on sensor deployment has focused on target tracking [5, 22], constrained coverage [16, 13, 19], repair and maintenance [1], and topology control for adaptive sampling [2, 20], usually with energy constraints in mind. We address here a variant of the topology control problem, assuming that sensors are autonomously mobile. Specifically we are interested in the problem of deploying sensors such that the resultant deployed sensor density follows the spatial variation of a scalar field in the environment. We are motivated by direct applications to environmental monitoring, e.g., the vertical temperature profile in the marine environment is thought to directly correlate to the abundance of microorganisms. If a system of sensors is to be deployed to maximum effect to measure microorganism abundance it would be prudent to try to exploit this fact by measuring temperature and deploying accordingly.

The Problem: In this paper we address the following question: *How can an ensemble of mobile sensor nodes deploy itself so that the deployment density (i.e. nodes per unit area in the 2D case) varies spatially in proportion to a scalar field induced by a physical phenomenon?* If $f(\mathbf{x})$ denotes a scalar field, how can sensor nodes deploy themselves so that the density distribution of the nodes $g(\mathbf{x})$ is proportional to $f(\mathbf{x})$, i.e. $g(\mathbf{x}) = k \cdot f(\mathbf{x})$ for some constant k . $f(\mathbf{x})$ could be any scalar field that can be estimated from sensor readings (e.g., temperature).

Assumptions and Constraints: Our key assumptions are a. the induced field is not known before deployment, b. all nodes are localized in a common global reference frame, c. all nodes can communicate within a short range, d. each node can compute the density of nodes in a small neighborhood, and e. each node can autonomously navigate from its current location to a commanded goal location. We are interested in large scale applications, where hundreds or thousands of nodes are to be deployed. This makes careful surveying and placement difficult. With these constraints and assumptions in mind, we have developed an algorithm which achieves the goal of deploying sensor nodes in the desired manner.

Approach and Contributions: Our approach rests on the following observation. The deployment distribution we want to achieve is easily computable in the special case where the area to be covered is very small (i.e. linear dimensions on the order of the communication range of each node) such that within it there exists one node (call it the cluster head) which can communicate directly with all other nodes in the area. In this case, each node within the cluster could measure the field value at its location and communicate it to the cluster head. Using standard function approximation techniques (e.g., using sampling [9, 14]), the cluster head could then compute desired node locations within the neighborhood and transmit these to the nodes, which would move accordingly thereby achieving the desired deployment density profile. Our strategy is to randomly parti-

tion space into sufficiently small neighborhoods at each iteration of the algorithm. Within each neighborhood the redistribution process as described above is enacted. We prove that after sufficiently many iterations, the distribution of nodes approaches the desired profile in the overall region. We also demonstrate empirically that our strategy is noise tolerant. We substantiate our results using simulations, and perform some simple experiments in one dimension using small robotic nodes called robomotes.

2. Related Work

Coverage is an important criterion for the quality of service of a sensor network [15], and has thus received significant attention. One approach is to deploy extra sensors based on the information collected by the deployed sensors. In [5], extra sensors are deployed randomly in the area to be monitored if deployed sensors can not achieve the required coverage. The authors show that the cost of deployment can be minimized while achieving desired detection performance. In [1], a robot works in coordination with a sensor network. The sensor network assists the robot in navigation and the robot deploys additional sensors to maximize the sensor coverage of the network. The approach introduced in [12] always places new nodes on the boundary of the area not yet covered by the sensor network. This approach is able to find a suboptimal deployment solution while ensuring each node retains line-of-sight with another node. Another related work is adaptive beacon placement [4], which deploys extra beacons in a similar way. It assumes that the localization error at each location has been measured before a new beacon is deployed.

Another approach frequently used for mobile sensor network deployment is the potential field technique [16, 13]. In [19], the author introduced an approach to detect coverage holes with a Voronoi diagram. The potential field is one of the three algorithms proposed to repair the coverage hole. [22] applied the potential field technique in a centralized way. One powerful leader is used to calculate the field and generate the location for all other nodes. This algorithm assumes that the environment is static and known before deployment. A centralized algorithm with the same assumptions is presented in [18]. This algorithm is a heuristic search based on grid world, which is aimed at minimizing the number of sensors deployed while maintaining given performance. The algorithm presented in [21] also assumes a powerful fusion station to assign the number of nodes within each cell of the sensing field in order to minimize the estimation distortion. A sensor deployment strategy to maintain network connectivity was studied in [6]. A UAV was used for deploying sensor nodes and measuring network connectivity. If some desired connectivity was missing, additional nodes were deployed by the UAV to repair

the connection.

The algorithm in this paper is different from above approaches in the following ways: First, we aim at deploying sensor nodes according to a profile that can be derived from the measurement of an environmental quantity. Second, our algorithm is distributed and it can be applied to a system consisting of large number of nodes.

Perhaps the most similar prior work is reported in [3] where a family of distributed methods for mobile sensor network deployment are proposed. In [3] every node determines its final location according to its initial location and the event distribution; hence the motion of each node can be predicted by any other node. However, the approaches in [3] assume that the initial distribution is uniform and depend on every sensor node predicting the motion of other nodes, which may be expensive. To predict the motion, each node also needs to know the initial location of all other nodes and all nodes need to know and agree on the locations of all events. Such information must be flooded across the whole network. Our approach makes no assumptions on the initial distribution of the sensor nodes and no information flooding is needed.

3. Deployment Algorithm

In this section, we first present an algorithm for deploying sensor nodes in a small neighborhood such that the node density is proportional to a scalar field $f(\mathbf{x})$. Next, we describe a distributed algorithm for sensor deployment, which randomly divides the plane into small neighborhoods at each iteration.

3.1. Deployment Within a Small Neighborhood

This work is inspired by the particle filter technique [9, 14], which has been used extensively for localization in robotics [8]. When applied to robot localization, the density of samples/particles is used to represent the probability distribution function (PDF) of robot location. In our algorithm, each sensor node corresponds to one particle in the particle filter and the scalar field $f(\mathbf{x})$ corresponds to the probability distribution function. By using an algorithm similar to the re-sampling algorithm used in particle filters, we generate new locations for the sensors so that the density distribution of the nodes is $g(\mathbf{x}) = k \cdot f(\mathbf{x})$.

Recall that we assume a system where each node is able to move and localize itself. It is also assumed that each node is able to detect node density in its vicinity (e.g., by counting the messages sent from its neighbors).

Within a small neighborhood, one node is selected as cluster head such that all other nodes are able to communicate with the cluster head directly. At the beginning of the

algorithm, all nodes send their locations, local node densities and sensor readings to the cluster head. The cluster head first compute the estimation of the scalar field from the readings and locations of all nodes. Then it puts all the locations, including its own, into a set P . Each location \mathbf{x} in P is weighted $w(\mathbf{x}) = \frac{f'(\mathbf{x})}{d(\mathbf{x})}$, where $f'(\mathbf{x})$ is the estimation of the field at location \mathbf{x} and the local node density around \mathbf{x} is $d(\mathbf{x})$. Next, the cluster head generates a set of new locations by re-sampling from this weighted set P . The re-sampling selects with high probability locations \mathbf{x} that have a high weight associated with them. By doing so, the density of new locations approximates the estimated scalar field. It is obvious that some locations would be selected multiple times. This problem is solved by applying Gaussian noise to the selected locations. The cluster head assigns each node in the cluster to a new location. There are two options to assign locations. One is to minimize the energy consumed by the whole cluster. In this case, the assignment algorithm should find the solutions so that the sum of the distances the nodes need to move is minimized. The other option is to balance the energy consumption among different nodes. In this case, each node is assigned a priority to choose its next location. The less the energy left in the battery, the higher priority the node gets. Every node selects the location closest to its current location from the available locations. Finally, all nodes move to the assigned locations.

The details of the algorithm are shown in Algorithm 1. The inputs N , P , R and D are sent to the cluster head from all nodes in the cluster. N is the total number of nodes in the cluster; P is the set of current node locations \mathbf{x} ; R is the set of sensor readings; D is the set of estimated local node densities. In this algorithm, subroutine `Estimate()` is used to estimate the scalar field from the sensor readings and it can be user defined. This is to accommodate cases where the sensors do not directly measure the field of interest and their measurements need to be processed before the field can be estimated. Another subroutine `AssignLocations()` takes the new locations and assigns them to all nodes in the cluster.

3.2. Distributed Algorithm

On the basis of the centralized algorithm that operates within a cluster, we designed a distributed algorithm for sensor deployment. For the distributed algorithm, we assume that:

1. The centralized algorithm is able to deploy the sensor nodes (within a cluster) in the distribution of $k \cdot f(\mathbf{x})$, where $f(\mathbf{x})$ is the induced field;
2. $f(\mathbf{x}) \geq 0$ for any $\mathbf{x} \in S$ and $\int_S f(\mathbf{x})d\mathbf{x} \neq 0$, where S is the sensing field;
3. The total number of nodes N is very large.

Algorithm 1: Location reassignment within a cluster

```

input :  $N, P, R, D$ 
output: None
// Estimate the scalar field  $F$ 
 $F = \text{Estimate}(R)$ ;
for  $k = 1$  to  $N$  do
     $Q[k] = \sum_{i=1}^k \frac{F[i]}{D[i]}$ ;
     $T[k] = \text{Rand}()$ ;
end
 $T = \text{Sort}(T)$ ;
 $i = 1$ ;
 $j = 1$ ;
while  $i \leq N$  do
    if  $T[i] < Q[j]$  then
         $\text{Index}[i] = j$ ;
         $i = i + 1$ ;
    else
         $j = j + 1$ ;
    end
end
AssignLocations(Index);

```

The distributed algorithm first randomly partitions the sensing field into subareas (small neighborhoods). The nodes within subarea S_j form a cluster C_j and one node is selected as the head within each cluster C_j . The cluster head executes Algorithm 1 which redeploys the sensor nodes so that the density distribution is $k_j \cdot f(\mathbf{x})$ within each cluster. A new random partition is now chosen and the process is repeated until termination conditions are satisfied. The details of the algorithm are shown in Algorithm 2, where P , R and D have the same meaning as in section 3.1.

Algorithm 2: Deployment algorithm

```

 $i = 0$ ;
while termination conditions are not satisfied do
    Randomly partition the sensing field into small subareas  $S_j^i$ ;
    Select one cluster head from nodes within each subarea;
    Each node  $n$  within one subarea sends  $R[n]$ ,  $P[n]$  and  $D[n]$  to cluster head;
    Cluster heads generate new locations with the distribution  $g_j^i(\mathbf{x}) = k_j^i f(\mathbf{x})$ , where  $k_j^i$  is a constant for any  $\mathbf{x} \in S_j^i$ ;
    Assign each node a new position;
    all nodes move to new locations;
     $i = i + 1$ ;
end

```

When implementing the algorithm, we use the LEACH protocol [10] to randomly partition the sensing field into

subareas and the system into clusters. In this approach, each node first elects itself as a cluster head with a pre-defined probability. If one node elects itself as a cluster head, it broadcasts its location to its neighbors. Otherwise, the node listens to the messages from cluster heads, and selects the one closest to it as its cluster head. The node joins the corresponding cluster by sending a registration message to the cluster head. The region covered by each cluster is one subarea.

4. Analysis

It can be proved that the algorithms of the previous section result in a distribution of the nodes which approaches the required distribution $k_0 \cdot f(\mathbf{x})$ as the number of timesteps increases. Formally, we have Theorem 4.1.

Theorem 4.1 *If S is the area of operation, $f(\mathbf{x})$ is the induced field and $g(\mathbf{x})$ is the actual node density distribution, as $i \rightarrow \infty$, $k_j^i \rightarrow k_0$ for all j , where*

$$k_0 = \frac{\int_S g(\mathbf{x}) d\mathbf{x}}{\int_S f(\mathbf{x}) d\mathbf{x}}.$$

To prove this theorem, we need the following lemmas.

Lemma 4.2 *If $k_i = k_j$ for any i and j , then for any subarea, $k_i = k_0$.*

Proof Suppose $k_i = k$ for any i , where k is a constant. That is, $g(\mathbf{x}) = k \cdot f(\mathbf{x})$ for $\mathbf{x} \in S$. So, we have

$$\int_S g(\mathbf{x}) d\mathbf{x} = \int_S k \cdot f(\mathbf{x}) d\mathbf{x} = k \cdot \int_S f(\mathbf{x}) d\mathbf{x}.$$

Therefore

$$k = \frac{\int_S g(\mathbf{x}) d\mathbf{x}}{\int_S f(\mathbf{x}) d\mathbf{x}} = k_0.$$

Lemma 4.3 *Let S_i^j be a subarea at timestep i , S_j^{i+1} be a subarea at timestep $i+1$, and $\Delta S_{j,l}^{i+1} = S_j^{i+1} \cap S_l^i$ as shown in Fig 1, where $j \in \{1, 2, \dots, M_{i+1}\}$ and $l \in \{1, 2, \dots, M_i\}$, we have*

$$k_j^{i+1} = \sum_{l=1}^{M_i} k_j^i \cdot \frac{\Delta F_{j,l}^{i+1}}{F_j^{i+1}},$$

where $F_j^{i+1} = \int_{S_j^{i+1}} f(\mathbf{x}) d\mathbf{x}$ and $\Delta F_{j,l}^{i+1} = \int_{\Delta S_{j,l}^{i+1}} f(\mathbf{x}) d\mathbf{x}$.

Proof According to Algorithm 2, after all nodes within S_j^{i+1} are redeployed,

$$g_j^{i+1}(\mathbf{x}) = k_j^{i+1} \cdot f(\mathbf{x}), \mathbf{x} \in S_j^{i+1}.$$

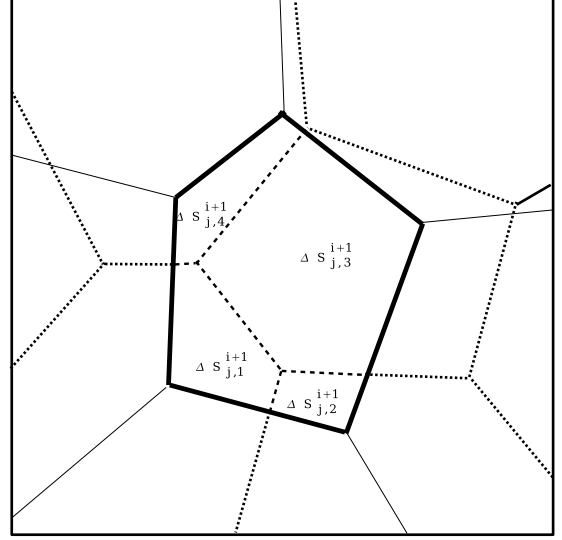


Figure 1. The dashed lines are the boundaries of the partitions at step i , and the solid lines are the boundaries at step $i+1$. The polygon with bold solid edges is subarea S_j^{i+1} . It is obvious that $S_j^{i+1} = \sum_{l=1}^{M_i} \Delta S_{j,l}^{i+1}$. Note that $\Delta S_{j,l}^{i+1}$ may be null for certain j or l .

Since $S_j^{i+1} = \sum_{l=1}^{M_i} \Delta S_{j,l}^{i+1}$, and the number of nodes in subarea S_j^{i+1} does not change after the redeployment, then

$$\int_{S_j^{i+1}} g_j^{i+1}(\mathbf{x}) d\mathbf{x} = N_j^{i+1} = \sum_{l=1}^{M_i} \int_{\Delta S_{j,l}^{i+1}} g_l^i(\mathbf{x}) d\mathbf{x}.$$

So, we have

$$\begin{aligned} k_j^{i+1} &= \frac{\int_{S_j^{i+1}} g_j^{i+1}(\mathbf{x}) d\mathbf{x}}{\int_{S_j^{i+1}} f(\mathbf{x}) d\mathbf{x}} \\ &= \frac{\sum_{l=1}^{M_i} \int_{\Delta S_{j,l}^{i+1}} g_l^i(\mathbf{x}) d\mathbf{x}}{\int_{S_j^{i+1}} f(\mathbf{x}) d\mathbf{x}} \\ &= \frac{\sum_{l=1}^{M_i} k_l^i \cdot \int_{\Delta S_{j,l}^{i+1}} f(\mathbf{x}) d\mathbf{x}}{\int_{S_j^{i+1}} f(\mathbf{x}) d\mathbf{x}} \\ &= \frac{\sum_{l=1}^{M_i} k_l^i \cdot \Delta F_{j,l}^{i+1}}{F_j^{i+1}}. \end{aligned}$$

Lemma 4.3 says that the proportionality constants associated with the distributions in subareas at the current step is the weighted average of the constants in previous step. Next, we prove that the difference between any two subareas will diminish after sufficiently many timesteps.

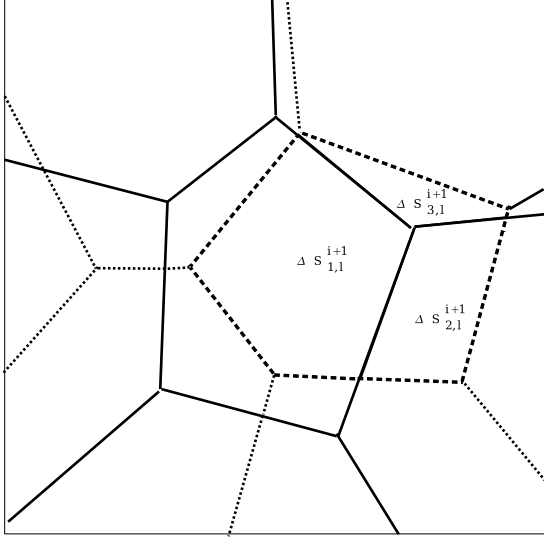


Figure 2. The dashed lines are the boundaries of subareas at step i , and solid lines are the boundaries of subareas at step $i + 1$. The polygon with bold dashed edges is the subspace S_l^i . It is obvious that $S_l^i = \sum_{j=1}^{M_{i+1}} \Delta S_{j,l}^{i+1}$.

Lemma 4.4 Let $\sigma^i = \sum_{l=1}^{M_i} \frac{F_l^i}{F} \cdot (k_l^i - k_0)^2$, where $F = \int_S f(\mathbf{x}) dx$ and $F_l^i = \int_{S_l^i} f(\mathbf{x}) dx$, then When step i approaches infinite, σ^i approaches 0.

Proof Since $S_l^i = \sum_{j=1}^{M_{i+1}} \Delta S_{j,l}^{i+1}$, as shown in Fig 2,

$$F_l^i = \int_{S_l^i} f(\mathbf{x}) dx = \sum_{j=1}^{M_{i+1}} \int_{\Delta S_{j,l}^{i+1}} f(\mathbf{x}) dx = \sum_{j=1}^{M_{i+1}} \Delta F_{j,l}^{i+1}.$$

For similar reason,

$$F_j^{i+1} = \sum_{l=1}^{M_i} \Delta F_{j,l}^{i+1}.$$

From the definition of σ^i , we have

$$\begin{aligned} \sigma^i &= \sum_{l=1}^{M_i} \frac{F_l^i}{F} (k_l^i - k_0)^2 \\ &= \sum_{l=1}^{M_i} \frac{\sum_{j=1}^{M_{i+1}} \Delta F_{j,l}^{i+1}}{F} (k_l^i - k_0)^2 \\ &= \frac{1}{F} \sum_{l=1}^{M_i} \sum_{j=1}^{M_{i+1}} [\Delta F_{j,l}^{i+1} (k_l^i - k_0)^2], \\ \sigma^{i+1} &= \sum_{j=1}^{M_{i+1}} \frac{F_j^{i+1}}{F} (k_j^{i+1} - k_0)^2. \end{aligned}$$

So, if we define $\Delta\sigma^i = \sigma^i - \sigma^{i+1}$,

$$\begin{aligned} \Delta\sigma^i &= \\ &= \frac{1}{F} \sum_{j=1}^{M_{i+1}} \left[\sum_{l=1}^{M_i} (k_l^i - k_0)^2 \Delta F_{j,l}^{i+1} - (k_j^{i+1} - k_0)^2 F_j^{i+1} \right]. \end{aligned}$$

Let

$$\begin{aligned} \alpha_j &= \sum_{l=1}^{M_i} (k_l^i - k_0)^2 \cdot \Delta F_{j,l}^{i+1}, \\ \beta_j &= (k_j^{i+1} - k_0)^2 \cdot F_j^{i+1} \end{aligned}$$

we have

$$\Delta\sigma^i = \frac{1}{F} \sum_{j=1}^{M_{i+1}} (\alpha_j - \beta_j).$$

On the other hand, replace l with l_1 ,

$$\begin{aligned} \alpha_j F_j^{i+1} &= \sum_{l_1=1}^{M_i} (k_{l_1}^i - k_0)^2 \Delta F_{j,l_1}^{i+1} F_j^{i+1} \\ &= \sum_{l_1=1}^{M_i} [(k_{l_1}^i - k_0)^2 \Delta F_{j,l_1}^{i+1} \left(\sum_{l_2=1}^{M_i} \Delta F_{j,l_2}^{i+1} \right)] \\ &= \sum_{l_1=1}^{M_i} \sum_{l_2=1}^{M_i} [(k_{l_1}^i - k_0)^2 \Delta F_{j,l_1}^{i+1} \Delta F_{j,l_2}^{i+1}], \end{aligned}$$

From lemma 4.3

$$\begin{aligned} \beta_j F_j^{i+1} &= (k_j^{i+1} - k_0)^2 (F_j^{i+1})^2 \\ &= [(k_j^{i+1} - k_0) \cdot F_j^{i+1}]^2 \\ &= \left[\sum_{l'=1}^{M_i} \Delta F_{j,l'}^{i+1} (k_{l'}^i - k_0) \right]^2. \end{aligned}$$

Then,

$$\begin{aligned} &(\alpha_j - \beta_j) \cdot F_j^{i+1} \\ &= \sum_{l_1=1}^{M_i} \sum_{l_2=1}^{M_i} \Delta F_{j,l_1}^{i+1} \Delta F_{j,l_2}^{i+1} [(k_{l_1}^i - k_0) - (k_{l_2}^i - k_0)]^2 \\ &= \sum_{l_1=1}^{M_i} \sum_{l_2=1}^{M_i} \Delta F_{j,l_1}^{i+1} \Delta F_{j,l_2}^{i+1} (k_{l_1}^i - k_{l_2}^i)^2. \end{aligned}$$

Therefore

$$\begin{aligned} \Delta\sigma^i &= \frac{1}{F} \sum_{j=1}^{M_{i+1}} (\alpha_j - \beta_j) \\ &= \frac{1}{F} \sum_{j=1}^{M_{i+1}} \left[\frac{1}{F_j^{i+1}} \sum_{l_1=1}^{M_i} \sum_{l_2=1}^{M_i} \Delta F_{j,l_1}^{i+1} \Delta F_{j,l_2}^{i+1} (k_{l_1}^i - k_{l_2}^i)^2 \right] \\ &= \frac{1}{F} \sum_{l_1=1}^{M_i} \sum_{l_2=1}^{M_i} \eta_{l_1,l_2}^{i+1} (k_{l_1}^i - k_{l_2}^i)^2, \end{aligned}$$

where $\eta_{l_1, l_2}^{i+1} = \sum_{j=1}^{M_{i+1}} \frac{\Delta F_{j, l_1}^{i+1} \cdot \Delta F_{j, l_2}^{i+1}}{F_j^{i+1}}$. Because $f(\mathbf{x}) \geq 0$, we have $F_j^{i+1} \geq 0$ and $\Delta F_{j, l}^{i+1} \geq 0$. Additionally, because $\Delta F_{j, l}^{i+1}$ are independent with step i , the probability that $\Delta F_{j, l}^{i+1} = 0$ for all j is very small, especially when there are large number of nodes in the system. So, we have $\Delta \sigma^i \geq 0$.

Now, we prove that σ^i approaches 0 as i approaches infinity. Suppose $\sigma^i \neq 0$ for any i . Since $\sigma^i \geq 0$, there must exist $\delta > 0$ so that for any i , $\sigma^i \geq \delta$. Suppose at step i , $(k_m^i - k_0)^2$ is the maximum among $(k_l^i - k_0)^2$ for all $l \in \{1, 2, \dots, M_i\}$, we have

$$\begin{aligned} \sigma^i &= \sum_{l=1}^{M_i} \frac{F_l^i}{F} (k_l^i - k_0)^2 \\ &\geq \frac{F_m^i}{F} (k_m^i - k_0)^2 \\ &\geq \delta. \end{aligned}$$

On the other hand, there must exist l' so that $(k_m^i - k_{l'}^i)^2 \geq (k_m^i - k_0)^2$. Then,

$$\begin{aligned} \Delta \sigma^i &\geq \frac{1}{F} \sum_{l_2=1}^{M_i} \eta_{m, l_2}^{i+1} (k_m^i - k_{l_2}^i)^2 \\ &\geq \frac{1}{F} \eta_{m, l'}^{i+1} (k_m^i - k_{l'}^i)^2 \\ &\geq \frac{1}{F} \eta_{m, l'}^{i+1} (k_m^i - k_0)^2 \\ &\geq \frac{1}{F} \eta_{m, l'}^{i+1} \frac{F}{F_m^i} \delta \\ &\geq \frac{\eta_{m, l'}^{i+1} (k_m^i - k_0)^2}{F_m^i} \delta \\ &\geq \eta_0 \delta, \end{aligned}$$

where $\eta_0 = \min_i \frac{\eta_{m, l'}^{i+1} (k_m^i - k_0)^2}{F_m^i}$ and $\eta_0 > 0$. So, if $i > \frac{\sigma^0 - \delta}{\eta_0 \cdot \delta}$, $\sigma^i < \delta$, which is a contradiction with the assumption that σ^i is always greater than or equal to δ hence the assumption is not true. Therefore, when i approaches infinity, σ^i approaches 0.

From Lemma 4.4, we can conclude that after sufficiently many steps, the k_j^i in all subareas are the same, and hence the density distribution of the nodes in the whole sensing field $g(\mathbf{x}) = k_0 \cdot f(\mathbf{x})$ for all $\mathbf{x} \in S$.

5. Simulation Results

We carried out several simulations to verify the validity of our algorithm. In the simulations, we assume that the scalar field is directly given by the readings $r(x, y)$ of sensors placed at locations (x, y) . We assumed a field which behaves as

$$r(x, y) = r_0(x, y) + \epsilon = 0.1 + e^{-\frac{(x-4)^2 + (y-6)^2}{2}} + \epsilon,$$

where ϵ is a zero-mean random variable with Gaussian distribution $N(0, \sigma)$.

The simulations were performed in a 2D environment of size 10x10. At the beginning of the simulations, all nodes are within a start area where $x \in [0, 1]$ and $y \in [0, 1]$. 500 nodes are deployed. The communication range of each node is 3 units. The probability that a node elects itself as a cluster head is chosen to be 0.05. Hence approximately 25 clusters are formed at each step.

Fig 3 shows the node densities after 120 steps in one simulation trial. One step here means one iteration of the redistribution process. Fig 3(a) is the scalar field and Fig 3(b) shows the node density distribution. In this trial, the covariance of the noise is 0.1, approximately 10% of the maximum reading.

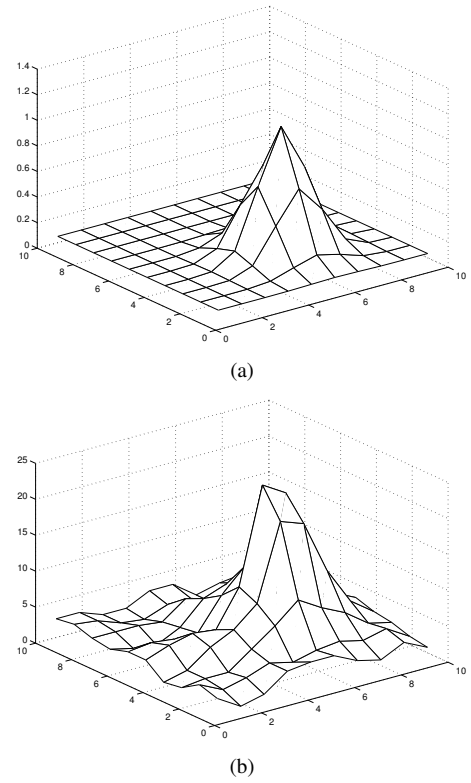


Figure 3. (a) the scalar field $f(\mathbf{x})$; (b) The node densities after 120 steps.

To illustrate the insensitivity of the algorithm to noise, we define desired node density, actual node density and density error as follows. Desired node density at location (x_0, y_0) is defined as

$$d_0(x_0, y_0) = \frac{\int_{(x,y) \in S} f(x, y) dx dy}{A},$$

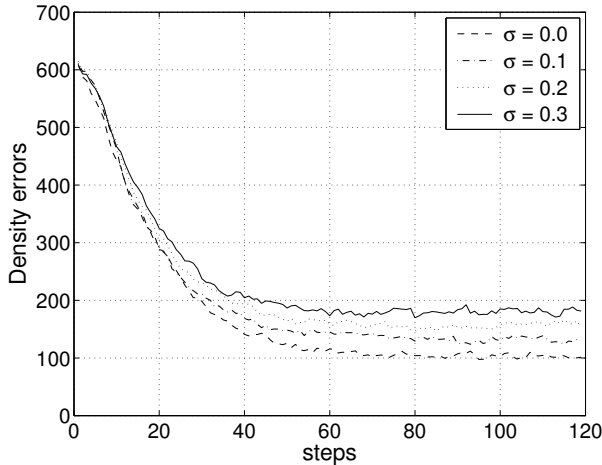


Figure 4. The node deployment density better approximates the desired profile over time. Shown here is the diminishing difference between the actual density and the desired density for different values of noise. The process is noise tolerant since there is little measurable difference between the steady-state density errors in four curves.

where s is a $\delta \times \delta$ square centered at (x_0, y_0) and $A = \delta^2$ is the area of s . In simulations, $\delta = 2.0$. Actual node density at location (x_0, y_0) is defined as

$$d(x_0, y_0) = \frac{n_s}{A},$$

where s and A have the same meaning as above and n is the number of nodes within the square s . The density error is defined as

$$err = \sum_{x \in \{0.5, 1.5, \dots, 9.5\}} \sum_{y \in \{0.5, 1.5, \dots, 9.5\}} |d(x, y) - d_0(x, y)|.$$

Fig 4 shows the density errors as a function of time. The simulations are done in 4 groups and each group consists of 10 trials. The trails in one group share the same noise covariance (σ), and each curve represents the average density errors over the trials within one group. From Fig 4 we can see that the error converges after about 60 steps. Note that in the simulations all nodes start from a small area and the convergence time includes the time for the nodes to expand to the whole sensing field. The convergence time and final steady-state error is largely insensitive to noise.

Fig 5 summarizes the steady-state density errors when the noise covariance increases from 0 to 0.4. Steady-state errors are computed by averaging the density errors after the 60th timestep. The basic observation is that our algorithm produces steady-state errors that increase slowly with the increase of the noise.

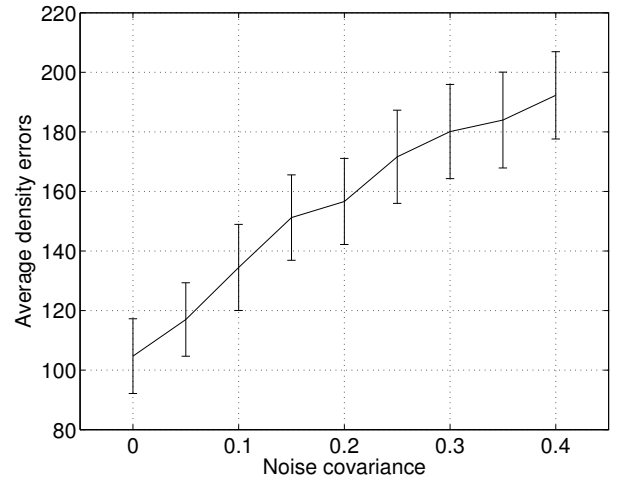


Figure 5. Steady-state density error increases slowly with increased sensor noise.

6. Physical Experiments

The sensor deployment algorithm has been tested on the Robomote robot testbed [7] (shown in Fig 6). The experiments are carried out on a $200cm \times 100cm$ table and Mezzanine [11] is used for node localization.

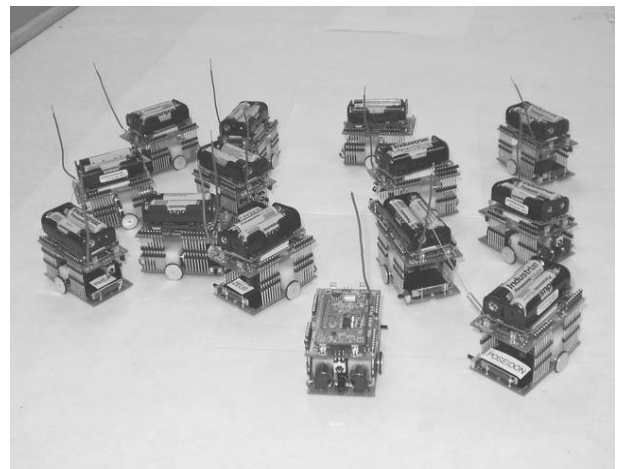


Figure 6. Robomote testbed

There are two implementation issues with the experiments on the robomote testbed. Given the small number (6) of robomotes available for experiments, the centralized algorithm may not deploy the nodes in the given distribution within each small neighborhood. That is, the density distribution of one time deployment may vary significantly from the desired profile. However, the average density distribu-

tion over several steps would approximate the desired one. Accordingly the average density distribution over the last 20 steps are used to display the experimental results. Another problem with a small number of nodes is an increased probability that no cluster is formed. For instance, in the experiments, the probability that one node elects itself as cluster head is set to be 0.25, so the probability that no cluster head is elected is $(1 - 0.25)^6 = 0.1780$. Since in the experiments the communication range is set to be 40 cm, the probability that one node does not join any cluster is even higher. Thus, some nodes might sit at one location for several steps. Because the overall node density is low (less than 1 per 10 cm), sitting at one location for even one step has considerable effect on the average density distribution. Therefore, each node is programmed to randomly move one step if it does not join any cluster. The other issue is that the size of a robomote is $7\text{cm} \times 4.5\text{cm}$ and hence the distance between two robomotes can not be very small. However, the new locations generated by the cluster head may be very close to each other. As a result, before assigning locations, the cluster heads check to make sure that the locations are such that the distance between any two locations is greater than a threshold.

Experiments with the robomotes were performed in one dimension. Robots were required to deploy themselves along the x-axis, based on measurements to a given profile

$$r(x) = e^{-\frac{(x-100)^2}{2 \cdot 30^2}},$$

and here we also assume that scalar field $f(x) = r(x)$. Several experiments were conducted, and the following are two selected examples. At the beginning of the experiments, all nodes start from the right boundary of the sensing field. Then, most nodes move away from their start locations towards the center of the sensing field and finally accumulate around the location $x = 100\text{cm}$. Fig 7 compares the final density distributions (bars) and the desired distribution (solid line, obtained by normalizing $f(x)$). The two distributions are in reasonable agreement.

7. Conclusion

In this paper, we presented a distributed deployment algorithm for a mobile sensor network which is able to deploy sensor nodes in a distribution proportional to a scalar field (induced by some environmental phenomenon). Our strategy is to randomly partition space into sufficiently small neighborhoods at each iteration of the algorithm. Within each neighborhood the redistribution process directed by a cluster head or leader node is enacted. We prove that after sufficiently many iterations, the distribution of nodes approaches the desired profile in the overall region.

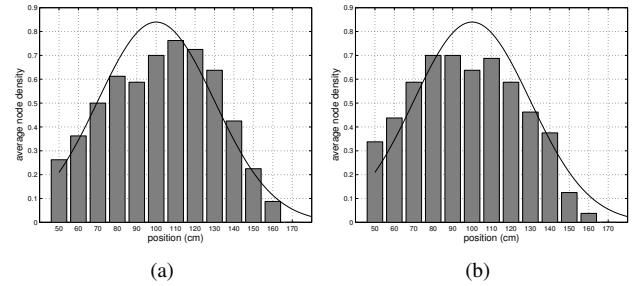


Figure 7. Data from two trials with the robomotes. The bars show the average sensor density distribution in the steady state, the curve shows the desired profile.

Though the algorithm partitions the system into clusters and each cluster needs one head, the cluster heads are selected randomly. So the algorithm does not suffer from single point failure. Another advantage of this algorithm is that sophisticated data fusion can be done by the cluster head since it has the sensing data from all its neighbors. For example, a cluster head may exploit linear regression to filter noise or identify failed nodes. We show experimentally that the algorithm is noise tolerant. Finally, the algorithm can be easily extended to 3D deployment as long as enough nodes are available. The experiments reported here are conducted in 1D and the simulations in 2D, but the algorithm does not make any assumption about the dimension of the problem.

The computational complexity depends on the number of nodes within each cluster. Given the size of the sensing field, the bigger the size of clusters, the faster the distributed algorithm converges while more computation is needed at each cluster head. The convergence speed of the distributed algorithm also depends on how the clusters are formed. More steps are needed if the system generates similar clusters at consecutive timesteps. Therefore, the algorithm could be improved by using a better cluster generating algorithm.

Acknowledgment

The authors thank Karthik Dantu and Sandeep Babel for their help with the robomote test bed and Aristides A. Requicha, David Caron, Amit Dhariwal and Beth Stauffer for their comments. This work is supported in part by the National Science Foundation (NSF) under grants CNS-0325875, IIS-0133947, EIA-0121141 and grants CCR-0120778, ANI-00331481 (via subcontract).

References

- [1] M. Batalin and G. S. Sukhatme. Coverage, exploration and deployment by a mobile robot and communication network. *Telecommunication Systems Journal, Special Issue on Wireless Sensor Networks*, 26(2):181–196, 2004.
- [2] M. A. Batalin, M. Rahimi, Y. Yu, D. Liu, A. Kansal, G. S. Sukhatme, W. J. Kaiser, M. Hansen, G. J. Pottie, M. Srivastava, and D. Estrin. Call and response: experiments in sampling the environment. In *Proceedings of the 2nd international conference on Embedded networked sensor systems*, pages 25–38. ACM Press, 2004.
- [3] Z. Bulter and D. Rus. Controlling mobile sensors for monitoring events with coverage constraints. In *Proc. of the IEEE International Conference on Robotics & Automation*, pages 1568–1573, 2004.
- [4] N. Bulusu, D. Estrin, L. Girod, and J. Heidemann. Scalable coordination for wireless sensor networks: Self-configuring localization systems. In *Proceedings of the Sixth International Symposium on Communication Theory and Applications (ISCTA '01)*, page xxx. University of California, Los Angeles, July 15-20th 2001.
- [5] T. Clouqueur, V. Phipatanasuphorn, P. Ramanathan, and K. K. Saluja. Sensor deployment strategy for target detection. In *Proceedings of the 1st ACM international workshop on Wireless sensor networks and applications*, pages 42–48. ACM Press, 2002.
- [6] P. I. Corke, S. E. Hrabar, R. Peterson, D. Rus, S. Saripalli, and G. S. Sukhatme. Autonomous deployment and repair of a sensor network using an unmanned aerial vehicle. In *IEEE International Conference on Robotics and Automation*, pages 3602–3609, Apr 2004.
- [7] K. Dantu, M. Rahimi, H. Shah, S. Babel, A. Dhariwal, and G. Sukhatme. Robomote: Enabling mobility in sensor networks, 2004.
- [8] F. Dellaert, D. Fox, W. Burgard, and S. Thrun. Monte carlo localization for mobile robots. In *Proc. of the IEEE International Conference on Robotics & Automation*, pages 1322–1328, 1999.
- [9] N. Gordon, D. Salmond, and A. Smith. Novel approach to nonlinear/non-gaussian bayesian state estimation. In *IEE Proceedings F of Radar and Signal Processing*, pages 107–113, 1993.
- [10] W. R. Heinzelman, A. Chandrakasan, and H. Balakrishnan. Energy-efficient communication protocol for wireless microsensor networks. In *HICSS*, 2000.
- [11] A. Howard. Mezzanine user manual; version 0.00, 2002.
- [12] A. Howard, M. J. Matarić, and G. S. Sukhatme. An incremental self-deployment algorithm for mobile sensor networks. *Autonomous Robots Special Issue on Intelligent Embedded Systems*, 13(2):113–126, 2002.
- [13] A. Howard, M. J. Matarić, and G. S. Sukhatme. Network deployment using potential fields: A distributed, scalable solution to the area coverage problem. In *Proceedings of the International Symposium on Distributed Autonomous Robotic Systems*, Jun 2002.
- [14] M. Isard and A. Blake. Condensation - conditional density propagation for visual tracking. *International Journal of Computer Vision*, (29(1)):5–28, 1998.
- [15] S. Meguerdichian, F. Koushanfar, M. Potkonjak, and M. B. Srivastava. Coverage problems in wireless ad-hoc sensor networks. In *INFOCOM*, pages 1380–1387, 2001.
- [16] S. Poduri and G. S. Sukhatme. Constrained coverage for mobile sensor networks. In *IEEE International Conference on Robotics and Automation*, pages 165–172, New Orleans, LA, May 2004.
- [17] D. O. Popa, A. C. Sanderson, R. Komerska, S. Muppapurapu, D. R. Blidberg, and S. Chappel. Adaptive sampling algorithms for multiple autonomous underwater vehicles. In *IEEE Autonomous Underwater Vehicles Workshop*, June 2004.
- [18] K. C. Santpal S. Dhillon and S. S. Iyengar. Sensor placement for grid coverage under imprecise detections. In *Proceedings of International Conference on Information Fusion*, pages 1581–1587, 2002.
- [19] G. Wang, G. Cao, and T. L. Porta. Movement-assisted sensor deployment. In *Proceedings of 23rd International Conference of IEEE Communications Society*, Mar 2004.
- [20] R. Willett, A. Martin, and R. Nowak. Backcasting: Adaptive sampling for sensor networks. In *Proceedings of the third international symposium on Information processing in sensor networks*, 2004.
- [21] X. Zhang and S. B. Wicker. How to distribute sensors in a random field? In *Proceedings of the third international symposium on Information processing in sensor networks*, pages 243–250. ACM Press, 2004.
- [22] Y. Zou and K. Chakrabarty. Sensor deployment and target localization in distributed sensor networks. *Trans. on Embedded Computing Sys.*, 3(1):61–91, 2004.